

Soft gluon resummation for gluon fusion ZH production

Goutam Das,^a Chinmoy Dey,^b M. C. Kumar^b and Kajal Samanta^c

^a*Institut für Theoretische Teilchenphysik und Kosmologie,
RWTH Aachen University, D-52056 Aachen, Germany*

^b*Department of Physics, Indian Institute of Technology Guwahati,
Guwahati-781039, Assam, India*

^c*Institute for Particle Physics Phenomenology,
Durham University, Durham DH1 3LE, United Kingdom*

E-mail: goutam@physik.rwth-aachen.de, d.chinmoy@iitg.ac.in,
mckumar@iitg.ac.in, kajal.samanta@durham.ac.uk

ABSTRACT: We examine the effects of soft gluons on Higgs boson production in association with a Z boson at the Large Hadron Collider (LHC). Utilizing the universal cusp anomalous dimensions and splitting kernels, we analyze effects of soft gluons on the gluon fusion ZH process, focusing on the total production cross-section as well as the invariant mass distribution at the next-to-leading logarithmic level. Additionally, we estimate the next-to-soft effects on this subprocess to the same level of accuracy. A detailed phenomenological analysis is performed for the 13.6 TeV LHC. Finally, combining these results with those from other subprocesses, we provide comprehensive predictions for the ZH production cross-section and the invariant mass distribution that will be valuable for comparison with experimental data from the upcoming LHC run as well as the future hadron colliders.

KEYWORDS: Resummation, Higgs Physics

¹TTK-24-58, P3H-24-100, IPPP/24/81

Contents

1	Introduction	1
2	Theoretical Framework	3
3	Numerical Results	7
3.1	Invariant mass distribution	8
3.2	Total cross-section	12
4	Conclusion	14

1 Introduction

The discovery of the Higgs boson [1–3] at the Large Hadron Collider (LHC) [4, 5] marks a significant milestone in particle physics. Following this breakthrough, the primary focus of the LHC has been the precise measurement of the Higgs boson’s properties and couplings. Such efforts not only deepen our understanding of the Higgs boson itself but also open new avenues for exploring physics beyond the Standard Model (BSM). Many BSM scenarios predict weak couplings to the Higgs boson at collider energies in the TeV range. Evidence of such interactions may manifest as deviations in total cross-sections or distributions for Higgs boson processes. Therefore, precise experimental measurements, combined with accurate theoretical predictions, are critical for identifying potential BSM signatures. The associated Higgs production with a vector boson at the LHC is of particular importance in probing Higgs coupling to the weak gauge bosons. Furthermore, it is crucial to constrain the sign of the top quark Yukawa coupling and examine its CP structure [6–8]. Keeping in mind the importance of this process, the ATLAS and CMS experiments are actively conducting precise measurements for this process [9–19]. Precise theoretical predictions are thus essential to complement the improved experimental results for this channel.

At the LHC, the Higgs boson is produced in association with Z boson primarily through the Drell-Yan (DY) type subprocess ($q\bar{q} \rightarrow Z^* \rightarrow ZH$) at the leading order (LO) in the strong coupling (α_s) expansion. The higher order Quantum Chromodynamics (QCD) correction for this channel thus closely follow the DY process and has been computed up to next-to-next-to leading order (N2LO) [20–27] and recently to next-to-next-to-next-to leading order (N3LO) [28] accuracy. The perturbative series for the DY-type contribution converges very quickly with next-to-leading order (NLO) amounting to around 30% correction to LO, whereas N2LO, N3LO receive around 3%, -0.8% corrections respectively relative to preceding orders. Additionally, the conventional theoretical scale uncertainty reduces to sub-percent level. The ZH process also gets a contribution from the bottom quark annihilation through the t -channel diagrams at the LHC. This involves a bottom Yukawa

coupling (y_b) and its contribution is found [29] to be at the sub-percent level. Furthermore, the Electro-Weak (EW) effects for this DY-type process have been computed to NLO [30] and a correction of around -5% was observed compared to the NLO QCD result. When fiducial cuts are applied, these corrections can grow significantly, reaching -10% to -20% of the NLO QCD distributions [31].

Compared to the DY process, the ZH process receives additional QCD contributions starting from N2LO. One such contribution involves Feynman diagrams where the Higgs boson is radiated from the massive top quark loop in the quark annihilation subprocess. Their contribution has been estimated [32] to be below 3% . Another type of subprocess which appear for the first time at N2LO i.e. at $\mathcal{O}(\alpha_s^2)$ is the ZH production through gluon fusion. Although the gluon fusion subprocess for ZH production is suppressed by two orders of strong couplings compared to the quark-antiquark annihilation subprocess, the suppression, however, is compensated considerably by the large gluon flux at the LHC. Therefore, starting from N2LO, this subprocess contributes dominantly. Due to its importance, the gluon fusion subprocess is being studied in great detail in the literature. The leading order of this subprocess (which contributes to $\mathcal{O}(\alpha_s^2)$) is a loop-induced process where ZH is produced through massive quark loop with top quark giving the dominant contributions. The LO of this subprocess has been computed with exact top quark mass in [33, 34] and is shown to provide correction of around 7% compared to the NLO QCD DY-type contribution (in contrast, the N2LO QCD DY-type contributes only around 3% compared to NLO DY) with a scale uncertainty of around 25% .

Several efforts were made to further improve the accuracy for gluon subprocess by calculating its NLO ($\mathcal{O}(\alpha_s^3)$) contribution. This requires computation of two-loop amplitudes involving multiple scales, including three masses: the Higgs boson mass (M_H), the Z boson mass (M_Z), and the top quark mass (m_t) as well as two Mandelstam variables. The presence of these large number of scales significantly increases the computational complexity. However, the calculation becomes significantly simpler in the infinite top-mass limit (EFT), where the NLO correction has been computed [35] within the framework of this EFT approximation for this subprocess. Nevertheless, there are continuous efforts to take into consideration of full mass dependence. The NLO real and virtual contributions have been computed using an asymptotic expansion of the top-quark mass [36]. Additionally, two-loop amplitudes have been evaluated through a high-energy and large- m_t expansion, utilizing the Padé approximation [37], as well as through a transverse momentum expansion [38]. The combined effects of the high-energy expansion and transverse momentum expansion were further explored in [39, 40]. The NLO cross-section and invariant mass distribution have also been obtained by incorporating the full top-mass dependence, alongside a small-mass expansion for M_H and M_Z [41]. More recently, two-loop virtual corrections have been computed with full top-mass effects [42], followed by a determination of the cross-section with full top-mass dependence at NLO in [43]. The total cross-section at NLO shows an approximately 100% increase compared to the LO result, with the scale uncertainty reduced to around 15% . In contrast, the distributions like transverse momentum of the Higgs boson, within the fiducial volume can exhibit corrections as large as a factor of 10.

The fixed order results for this subprocess still suffer from the large threshold logarithms

arising from soft gluons emission. These large logarithms need to be resummed to have reliable predictions. The size of the NLO corrections indicates that this subprocess will receive significant contributions from the threshold logarithms similar to the Higgs case. Resummation of these large soft (SV) logarithms is well-established in the literature [44–53] and have been applied to many colorless processes [54–57, 57–69] leading to improved predictions for inclusive cross-sections and invariant mass distributions. Recently, efforts were made to incorporate the next-to-soft (NSV) threshold effects for colorless productions [70–81]. For the ZH production in the DY-type channel, the effects of soft gluons have been estimated in [82] to next-to-next-to-next-to-leading logarithmic (N3LL) accuracy matched to N3LO fixed order in QCD. A better perturbative convergence has been observed for threshold resummation for invariant mass distribution of ZH pair. For the gluon fusion ZH process, the effects of soft gluons have been studied [83] for the total cross-section to next-to-leading logarithmic (NLL) accuracy matched to NLO in QCD in the EFT approximation where a correction about 15% of NLO was obtained. Similar accuracy for the invariant mass distribution is still missing.

The goal of this paper is to improve the gluon fusion ZH process by incorporating soft and next-to-soft gluon resummation for both the total cross-section and the invariant mass distribution of the ZH pair. We work in the exact Born-improved gluon fusion channel, which has been shown to work effectively for the Higgs case, and we expect similar behavior for the ZH process. For NSV resummation, we closely follow the approach outlined in [78, 79]. Additionally, we present the complete result at $\mathcal{O}(\alpha_s^3)$, improved with SV threshold resummation from both quark and gluon channels for ZH production.

The article is organized as follows: In Section 2, we introduce the key theoretical formulas and present the coefficients required for performing SV and NSV resummation up to the necessary order. In Section 3, we provide a phenomenological study for the gluon fusion subprocess, combining it with the DY-type contributions to present complete results for pp collisions at $\mathcal{O}(\alpha_s^3)$ accuracy. Finally, we conclude in Section 4.

2 Theoretical Framework

The hadronic cross-section for ZH production in proton collision is provided in QCD factorization as,

$$Q^2 \frac{d\sigma}{dQ^2} = \sum_{a,b} \int_0^1 dx_1 \int_0^1 dx_2 f_a(x_1, \mu_F^2) f_b(x_2, \mu_F^2) \int_0^1 dz \delta(\tau - zx_1x_2) Q^2 \frac{d\hat{\sigma}_{ab}(z, \mu_F^2)}{dQ^2}, \quad (2.1)$$

where $f_{a,b}$ are the parton distribution functions (PDFs) for parton a, b in the incoming hadrons and $\hat{\sigma}_{ab}$ is the partonic coefficient function. The hadronic and partonic threshold variables $\tau = Q^2/S$ and $z = Q^2/\hat{s}$ are defined in terms of respective center-of-mass energies S and \hat{s} . Here Q is the invariant mass of the ZH system and μ_F is the factorisation scale. The partonic coefficient function can be decomposed (suppressing all scale dependencies)

as,

$$Q^2 \frac{d\hat{\sigma}_{ab}(z)}{dQ^2} = \hat{\sigma}_{ab}^{(0)}(Q^2) \left(\delta_{ba} \Delta_{ab}^{\text{SV}}(z) + \Delta_{ab}^{\text{REG}}(z) \right). \quad (2.2)$$

The term Δ_{ab}^{SV} appears only for the diagonal subprocesses $(gg, q\bar{q})$ and is known as the soft-virtual (SV) partonic coefficient and it captures the leading singular terms in the $z \equiv 1 - \bar{z} \rightarrow 1$ limit. The Δ_{ab}^{REG} term, on the other hand, contains subleading or regular contributions in the variable z . In general, they follow the expansion in the strong coupling at the renormalisation scale $\alpha_s(\mu_R^2) \equiv 4\pi a_s(\mu_R^2)$ as,

$$\begin{aligned} \Delta_{ab}^{\text{SV}}(z) &= \sum_{n=0}^{\infty} a_s^n(\mu_R^2) \delta_{ab} \left(\Delta_{\delta}^{(n)} \delta(\bar{z}) + \sum_{k=0}^{2n-1} \Delta_{\mathcal{D}_k}^{(n)} \mathcal{D}_k(\bar{z}) \right), \quad \text{with } ab \in \{gg, q\bar{q}\}, \quad (2.3) \\ \Delta_{ab}^{\text{REG}}(z) &= \Delta_{ab}^{\text{NSV}}(z) + \sum_{n=0}^{\infty} a_s^n(\mu_R^2) \Delta_{ab}^{(n)}(z) = \sum_{n=0}^{\infty} a_s^n(\mu_R^2) \left(\sum_{k=0}^{2n-1} \Delta_{ab, \ln_k}^{(n)} \ln^k(\bar{z}) + \Delta_{ab}^{(n)}(z) \right), \end{aligned}$$

where $\delta(\bar{z})$ is the Dirac delta distribution and $\mathcal{D}_k(\bar{z}) \equiv [\ln^k(\bar{z})/\bar{z}]_+$ are the plus-distributions. At the leading order, all the coefficients vanish except $\Delta_{\delta}^{(0)} = 1$. Here $\Delta_{ab, \ln_k}^{(n)}$ are the next-to-soft (NSV) coefficients which get contributions from both diagonal as well as off-diagonal channels. The last term in the above expression $\Delta_{ab}^{(n)}(z)$ vanishes in the soft limit $\bar{z} \equiv 1 - z \rightarrow 0$. Note that the singular SV part of the partonic coefficient has a universal structure which gets contributions from the underlying hard form factor, mass factorization kernels [84, 85] and soft radiations [49, 50, 86–89]. All of these are infrared divergent which however when regularized and combined give finite contributions.

The Born normalization factor $\hat{\sigma}_{ab}^{(0)}$ in Eq. (2.2) takes the following form for $q\bar{q}$ subprocess,

$$\hat{\sigma}_{q\bar{q}}^{(0)}(Q^2) = \left(\frac{\pi \alpha^2}{n_c S} \right) \left[\frac{M_Z^2 \lambda^{1/2}(Q^2, M_H^2, M_Z^2) \left(1 + \frac{\lambda(Q^2, M_H^2, M_Z^2)}{12 M_Z^2 / Q^2} \right)}{(Q^2 - M_Z^2)^2 c_w^4 s_w^4} \left((g_q^V)^2 + (g_q^A)^2 \right) \right], \quad (2.4)$$

with $g_a^A = -\frac{1}{2} T_a^3$, $g_a^V = \frac{1}{2} T_a^3 - s_w^2 Q_a$, Q_a being the electric charge and T_a^3 being the weak isospin of the fermions. Here, α is the fine structure constant, s_w, c_w are the sine and cosine of the Weinberg angle respectively, and $n_c = 3$ in QCD. M_Z and M_H are the masses of the Z boson and Higgs boson respectively and the function λ is defined as $\lambda(z, y, x) = (1 - x/z - y/z)^2 - 4xy/z^2$.

For the gluon fusion subprocess, in the infinite top mass limit, the Born factor takes the form [35],

$$\hat{\sigma}_{gg}^{(0), \text{EFT}}(Q^2) = \left(\frac{\sqrt{\pi} a_s(\mu_R^2) \alpha}{16 s_w^2 c_w^2} \right)^2 \left(\frac{Q^2}{M_Z^4} \right) \lambda^{\frac{3}{2}}(Q^2, M_H^2, M_Z^2). \quad (2.5)$$

In the infinite top mass approximation, the full NLO correction to the gluon fusion subprocess is known [35]. In particular, the SV and NSV coefficients up to NLO are given

as,

$$\begin{aligned}
\Delta_\delta^{(1)} &= \left(\frac{56}{27} + 8\zeta_2 \right) C_A + \frac{64}{9} T_F n_f + \left(\frac{46}{9} C_A - 2\beta_0 \right) \ln \left(\frac{\mu_F^2}{Q^2} \right) - 2\beta_0 \ln \left(\frac{\mu_F^2}{\mu_R^2} \right) \\
&\quad + \frac{\widehat{\sigma}_{(\text{virt,red})}}{a_s(\mu_R^2) \widehat{\sigma}_{gg}^{(0),\text{EFT}}(Q^2)}, \\
\Delta_{\mathcal{D}_0}^{(1)} &= -\Delta_{gg,\ln_0}^{(1)} + 8C_A = -8C_A \ln \left(\frac{\mu_F^2}{Q^2} \right), \\
\Delta_{\mathcal{D}_1}^{(1)} &= -\Delta_{gg,\ln_1}^{(1)} = 16C_A.
\end{aligned} \tag{2.6}$$

Here $\widehat{\sigma}_{(\text{virt,red})}$ is the ‘‘virtual reducible’’ contribution arising from Feynman diagrams involving two quark triangles which in the infinite top mass limit takes the form [35],

$$\begin{aligned}
\widehat{\sigma}_{(\text{virt,red})} &= \int d\widehat{t} a_s(\mu_R^2) \frac{4}{3} \left(\frac{\sqrt{\pi} a_s(\mu_R^2) \alpha}{16s_w^2 c_w^2} \right)^2 \frac{1}{\widehat{s} M_Z^4} \\
&\quad \times \left\{ M_H^2 \left(-1 + \frac{M_Z^2}{\widehat{t} - M_Z^2} + \ln \left(\frac{-\widehat{t}}{M_Z^2} \right) \frac{M_Z^2}{\widehat{t} - M_Z^2} - \ln \left(\frac{-\widehat{t}}{M_Z^2} \right) \frac{M_Z^4}{(\widehat{t} - M_Z^2)^2} \right) \right. \\
&\quad \left. + (\widehat{s} - M_Z^2) \left(-1 - \frac{M_Z^2}{\widehat{t} - M_Z^2} + \ln \left(\frac{-\widehat{t}}{M_Z^2} \right) \frac{\widehat{t} M_Z^2}{(\widehat{t} - M_Z^2)^2} \right) + (\widehat{t} \leftrightarrow \widehat{u}) \right\}, \tag{2.7}
\end{aligned}$$

where \widehat{u}, \widehat{t} are the partonic Mandelstam variables.

The born coefficient in the exact theory, on the other hand, contains Feynman diagrams involving triangle and box diagrams with heavy top quark dependence. It can be expressed in terms of helicity amplitudes for triangle and box diagrams as,

$$\widehat{\sigma}_{gg}^{(0)}(Q^2) = \left(\frac{\sqrt{\pi} a_s(\mu_R^2) \alpha}{16s_w^2} \right)^2 \frac{1}{8\widehat{s}^2} \int d\widehat{t} \sum_{\lambda_g, \lambda'_g, \lambda_Z} \left| \mathcal{M}_{\lambda_g \lambda'_g \lambda_Z}^\Delta + \mathcal{M}_{\lambda_g \lambda'_g \lambda_Z}^\square \right|^2. \tag{2.8}$$

The exact expression for these helicity amplitudes for two gluons and a Z boson can be found in [34]. These large distributions appearing in the Δ^{SV} can be resummed to all orders in the threshold limit $z \rightarrow 1$. Typically, resummation is performed in the Mellin N -space where plus-distributions become simple logarithm in Mellin variable (N). The threshold limit $z \rightarrow 1$ translates into $N \rightarrow \infty$ limit. Recently a formalism has been proposed [78–80, 90, 91] to also resum the NSV logarithms arising out of the diagonal channel. Essentially the partonic SV and NSV coefficients in the Mellin space can be organized as follows,

$$\frac{1}{\widehat{\sigma}_{ab}^{(0)}(Q^2)} Q^2 \frac{d\widehat{\sigma}_{N,ab}^{\overline{\text{NNLL}}}}{dQ^2} = \int_0^1 dz z^{N-1} (\Delta_{ab}^{\text{SV}}(z) + \Delta_{ab}^{\text{NSV}}(z)) \equiv g_0(Q^2) \exp(G_N^{\text{SV}} + G_N^{\text{NSV}}). \tag{2.9}$$

The factor g_0 is independent of the Mellin variable and contains process-dependent information. The leading threshold enhanced large logarithms and the next-to soft logarithms

in Mellin space are resummed through the exponent G_N^{SV} and G_N^{NSV} respectively. The resummed accuracy is determined through the successive terms from both the exponent G_N which takes the form,

$$G_N^{\text{SV}} = \ln(\bar{N}) g_1(\omega) + \sum_{n=1}^{\infty} a_s^{n-1}(\mu_R^2) g_{n+1}(\omega),$$

$$G_N^{\text{NSV}} = \frac{1}{N} \sum_{n=0}^{\infty} a_s^n(\mu_R^2) \left(\bar{g}_{n+1}(\omega) + \sum_{k=0}^n h_{nk}(\omega) \ln^k \bar{N} \right), \quad (2.10)$$

where $\bar{N} = N \exp(\gamma_E)$ with γ_E being the Euler–Mascheroni constant and $\omega = 2\beta_0 a_s(\mu_R^2) \ln \bar{N}$. The first term in the expansion of G_N^{SV} corresponds to the leading logarithmic (LL) accuracy, whereas the inclusion of successive terms defines higher accuracies. These coefficients (g_n) are universal and only depend on the partonic flavours being either quark or gluon. In order to obtain $\overline{\text{LL}}$ accuracy in NSV resummation, one has to consider NSV exponents \bar{g}_1 and h_{00} in addition to the LL terms. Similarly, for higher accuracies, one has to consider the next terms in the expansion of G_N . Note that starting from NLL ($\overline{\text{NLL}}$), one has to also consider the N -independent g_0 coefficients whose perturbative expansion takes the form,

$$g_0(Q^2) = 1 + \sum_{n=1}^{\infty} a_s^n(\mu_R^2) g_{0n}(Q^2). \quad (2.11)$$

The explicit form of the resum exponent for SV and NSV resummation can be found *e.g.* in [47, 54]. Up to NLL($\overline{\text{NLL}}$) one requires the following coefficients,

$$g_1(\omega) = \frac{1}{\beta_0} \left\{ C_A \left(8 \left(1 + \frac{\bar{\omega}}{\omega} L_\omega \right) \right) \right\},$$

$$g_2(\omega) = \frac{1}{\beta_0^3} \left\{ C_A \beta_1 (4\omega + 4L_\omega + 2L_\omega^2) + C_A n_f \beta_0 \left(\frac{40}{9} (\omega + L_\omega) \right) \right. \\ \left. + C_A^2 \beta_0 \left(\left(-\frac{268}{9} + 8\zeta_2 \right) (\omega + L_\omega) \right) + C_A \beta_0^2 \left(4L_\omega \ln \left(\frac{Q^2}{\mu_R^2} \right) + 4\omega \ln \left(\frac{\mu_F^2}{\mu_R^2} \right) \right) \right\},$$

$$\bar{g}_1(\omega) = \frac{1}{\beta_0} \left\{ C_A (4L_\omega) \right\},$$

$$\bar{g}_2(\omega) = \frac{1}{\bar{\omega} \beta_0^2} \left\{ C_A C_F n_f (-8(\omega + L_\omega)) + C_A^2 n_f \left(-\frac{40}{3} (\omega + L_\omega) \right) + C_A^3 \left(\frac{136}{3} (\omega + L_\omega) \right) \right. \\ \left. + C_A n_f \beta_0 \left(\frac{40}{9} \omega \right) + C_A^2 \beta_0 \left(-\frac{268}{9} + 8\zeta_2 \right) \omega + C_A \beta_0^2 \left(-8 + 4 \ln \left(\frac{Q^2}{\mu_R^2} \right) - 4\bar{\omega} \ln \left(\frac{\mu_F^2}{\mu_R^2} \right) \right) \right\},$$

$$h_{00}(\omega) = \frac{1}{\beta_0} \left\{ C_A (-8L_\omega) \right\},$$

$$h_{10}(\omega) = \frac{1}{\bar{\omega} \beta_0^2} \left\{ C_A \beta_1 (-8(\omega + L_\omega)) + C_A n_f \beta_0 \left(-\frac{80}{9} \omega \right) + C_A^2 \beta_0 \left(\frac{536}{9} - 16\zeta_2 \right) \omega \right. \\ \left. + C_A \beta_0^2 \left(8 - 8 \ln \left(\frac{Q^2}{\mu_R^2} \right) + 8\bar{\omega} \ln \left(\frac{\mu_F^2}{\mu_R^2} \right) \right) \right\},$$

$$h_{11}(\omega) = \frac{1}{\bar{\omega}^2 \beta_0} \left\{ C_A^2 (32\omega \bar{\omega}^2 - 4\omega) \right\}, \quad (2.12)$$

where $\bar{\omega} = 1 - \omega$ and $L_\omega = \ln(\bar{\omega})$. Note that up to the required order $\overline{\text{NLL}}$, the SV and NSV exponents are the same as the ggH case. Up to NLL($\overline{\text{NLL}}$) accuracy, one also needs the coefficient g_{01} which for the gluon subprocess we found it to be,

$$g_{01}(Q^2) = \left(\frac{56}{27} + 16\zeta_2 \right) C_A + \frac{64}{9} T_F n_f - 2\beta_0 \ln \left(\frac{\mu_F^2}{\mu_R^2} \right) + \left(\frac{46}{9} C_A - 2\beta_0 \right) \ln \left(\frac{\mu_F^2}{Q^2} \right) + \frac{\hat{\sigma}_{(\text{virt,red})}}{a_s(\mu_R^2) \hat{\sigma}_{gg}^{(0)}(Q^2)}. \quad (2.13)$$

Note that both g_0 and G_N are scheme-dependent which is related to the ambiguity in exponentiation of certain constant terms (e.g. γ_E) coming from Mellin transformation along with the large- N terms (see e.g. [68] for a detailed discussion). In the context of LHC, it has been observed that the so-called \overline{N} -scheme provides a faster perturbative convergence for the resummed series. In this scheme, the constant g_0 is independent of γ_E .

The resummed result in Eq. (2.9) has to be finally matched with the available fixed order results to incorporate the hard regular contribution and, at the same time, avoid double counting of SV(NSV) logarithms. The matching with the fixed order is usually performed using the *minimal prescription* [92] and for \overline{NnLL} resummation it reads,

$$Q^2 \frac{d\sigma_{ab}^{\text{NnLO}+\overline{\text{NnLL}}}}{dQ^2} = Q^2 \frac{d\sigma_{ab}^{\text{NnLO}}}{dQ^2} + \sum_{ab \in \{gg, q\bar{q}\}} \hat{\sigma}_{ab}^{(0)}(Q^2) \int_{c-i\infty}^{c+i\infty} \frac{dN}{2\pi i} \tau^{-N} f_{a,N}(\mu_F) f_{b,N}(\mu_F) \times \left(Q^2 \frac{d\hat{\sigma}_{N,ab}^{\overline{\text{NnLL}}}}{dQ^2} - Q^2 \frac{d\hat{\sigma}_{N,ab}^{\overline{\text{NnLL}}}}{dQ^2} \Big|_{\text{tr}} \right). \quad (2.14)$$

Note that similar matching procedure is done for the SV resummation. The $f_{a,N}$ are the Mellin transformed PDF similar to the partonic coefficient in Eq. (2.9) and can be evolved e.g. using publicly available code QCD-PEGASUS [93]. However, for practical purposes, it can be also approximated by directly using z -space PDF following [45, 54]. The subscript ‘tr’ in the last term in the bracket in Eq. (2.14) denotes that the resummed partonic coefficient in Eq. (2.9) has been truncated to the fixed order to avoid double counting the terms already present in the fixed order through $\sigma_{ab}^{\text{NnLO}}$. Essentially, for SV resummation, this will contain all the fixed order singular logarithms and for NSV resummation, it will contain additional NSV terms from the diagonal channel. In the next section, we study the impact of SV and NSV resummation on the gluon subprocess at LHC.

3 Numerical Results

In this section, we present numerical results for ZH associated production at the LHC. The default center-of-mass energy of the incoming protons is set to 13.6 TeV. Unless specified otherwise, our numerical analysis employs the PDF4LHC21_40 [94] parton distribution functions (PDFs) throughout, as provided by LHAPDF [95]. In all these cases, the central set is the standard choice. The strong coupling is provided through the LHAPDF routine. The fine structure constant is taken as $\alpha \simeq 1/127.93$. The masses of the weak gauge bosons are set

to be $M_Z = 91.1880$ GeV and $M_W = 80.3692$ GeV [96] with the corresponding total decay widths of $\Gamma_Z = 2.4955$ GeV. The Weinberg angle is then given by $\sin^2\theta_w = (1 - m_W^2/m_Z^2)$. This corresponds to the weak coupling $G_F \simeq 1.2043993808 \times 10^{-5}$ GeV $^{-2}$. The mass of the Higgs boson is set to $M_H = 125.2$ GeV.

In the gluon fusion channel, only the top quark contribution is considered at the lowest order, with the top quark pole mass set to $m_t = 172.57$ GeV. For this case, we chose the pole mass of the bottom quark to be $m_b = 4.78$ GeV. The unphysical renormalization (μ_R) and factorization scales (μ_F) are set to the invariant mass (Q) of the ZH pair. The scale uncertainties are estimated by simultaneously varying these unphysical scales in the range $[Q/2, 2Q]$ keeping the constraint $|\ln(\mu_R/\mu_F)| < \ln 4$ (known as the 7-point scale uncertainty) and taking the maximum absolute deviation of the cross-section from that obtained with the central scale choice. To estimate the impact of the higher order corrections from FO and resummation, we define the following ratios of the cross-sections,

$$K_{nm} = \frac{\sigma^{\text{NnLO}}}{\sigma_c^{\text{NmLO}}}, R_{nm} = \frac{\sigma^{\text{NnLO+NnLL}}}{\sigma_c^{\text{NmLO}}} \text{ and } \bar{R}_{nm} = \frac{\sigma^{\text{NnLO+NnLL}}}{\sigma_c^{\text{NmLO}}}. \quad (3.1)$$

The subscript ‘ c ’ in the above expressions indicates that the corresponding quantity is evaluated at the central scale choice. As stated earlier, the lowest order process for ZH production through the gluon fusion channel contributes at $\mathcal{O}(\alpha_s^2)$ level, which formally should be considered at N2LO in the perturbation theory. Consequently, we have used the N2LO PDF for the computation of LO and higher order corrections to the gluon fusion process.

3.1 Invariant mass distribution

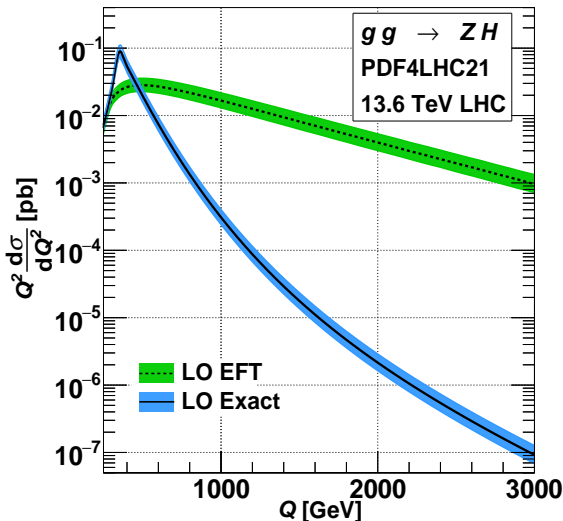


Figure 1: Invariant mass distribution of ZH for the gluon fusion channel at LO for EFT and Exact theories at 13.6 TeV LHC are presented. The bands correspond to the theoretical uncertainty using 7-point scale variation.

We first look into the invariant mass distribution of ZH pair. As mentioned in Section 1, the computation of higher-order corrections is non-trivial due to the involvement of multiple scales and one can work with EFT to reduce this complexity. For inclusive production of ZH pair, the total cross-section differs between these two approaches by around 31% at LO. However, the difference is more pronounced in the invariant mass distribution as can be seen from Fig. 1. The band in this plot corresponds to the 7-point scale uncertainty as described above. Although the differential cross-section is comparable in the low invariant mass region, the shape differs significantly in the higher invariant mass region. Therefore, it is essential to include the finite top quark mass effect to produce the correct behavior for the invariant mass distribution. On the other hand, the total cross-section with finite top quark mass effect at NLO differs only by 5% [43] from the same in EFT. In fact, the exact LO captures the shape of the distribution in bulk and the effect of top mass on the NLO correction will have less impact on the shape of the distribution. Therefore, working with a Born-improved theory where the LO is rescaled by the exact top quark effect and NLO corrections in the EFT, will reduce the complexity while retaining essential features of QCD corrections, in particular the effects of soft radiation where we are interested in. In the rest of the article, we use this exact Born-improved EFT NLO cross-section for all purposes.

The fixed order results¹ have been computed with the publicly available code `vh@nnlo` [23, 27, 35] and for resummation, we have developed an in-house code to handle the Mellin inversion described in the end of Section 2. We first verified our code by reproducing the known result for the total resummed cross-section for ZH production up to NLO+NLL [83] in the N -scheme. We further reproduced the known result for inclusive resummed Higgs cross-section up to NLO+NLL both in N - and \bar{N} -schemes. As discussed in Section 2, the \bar{N} -scheme offers a faster perturbative convergence with a better control on the scale uncertainty and we chose to use this scheme for all of our studies in this article.

On the left panel of Fig. 2, we compare the SV resummation with the fixed order result up to NLO(NLL) level, and we observe the expected behavior of better perturbative convergence for the SV resummed series. This is further evidenced from the lower inset where the ratios are displayed. From the ratio K_{10} , it is evident that the NLO correction can reach to around 100% compared to LO across most of the kinematic region considered. The LO+LL correction captures a significant portion of the higher order effects and provides an additional contribution of 80% of the LO, particularly in the high invariant mass region ($Q = 3000$ GeV). This clearly demonstrates that the soft gluon effect is dominant for this process. The NLO+NLL correction also shows a significant enhancement (through the R_{10} factor), reaching around 2.8 times the LO, particularly in the high invariant mass region. On the right panel of Fig. 2, we further compare the NLO(NLL) results with the new \bar{NLL} results. Through the ratios R_{11} and \bar{R}_{11} on the bottom panel there, we observe that NLO+NLL corrections account for about 20% of NLO in the low invariant mass region

¹At NLO with exact top quark dependence, there are also Z radiated diagrams where a Z boson is emitted from the external light quark line. These kind of diagrams will contribute to $\mathcal{O}(\alpha_s^3 y_t^2)$ (y_t being the top quark Yukawa coupling) i.e. the same order as the gluon fusion subprocess at exact NLO. Their effects could be as large as 10 times [40] the LO results.

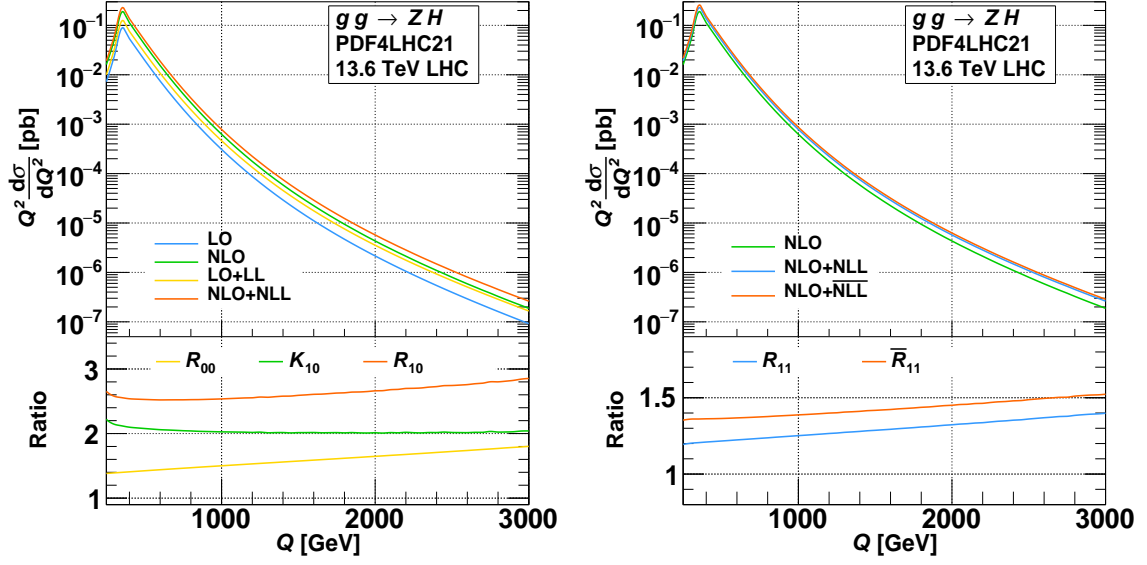


Figure 2: Comparison between the Born-improved fixed order and resummed results with corresponding ratios as defined in Eq. (3.1) are shown here. In the left panel; a comparison between fixed order and SV resummation are shown, and in the right panel; a comparison among fixed order, SV resummation and NSV resummation are presented.

and rise to approximately 40% in the high invariant mass region. The NSV resummation at NLO+NLL, on the other hand, contributes an additional 12% – 15% correction over NLO+NLL across most of the invariant mass region.

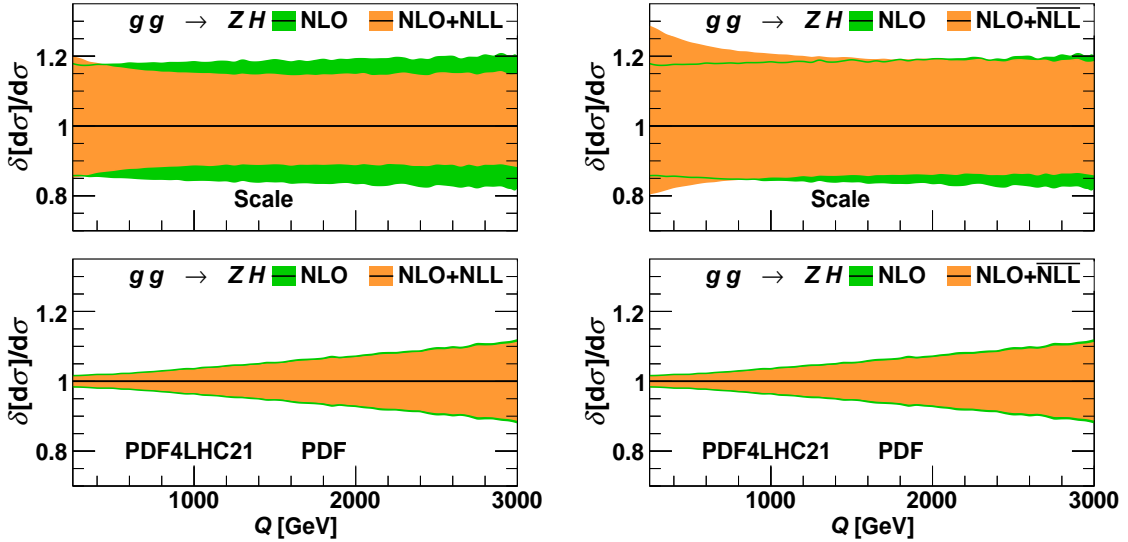


Figure 3: The 7-point scale uncertainty (upper panel) and the PDF uncertainty (lower panel) of gluon fusion ZH production are compared for Born-improved SV (left) and NSV resummation (right) against their corresponding fixed order results at 13.6 TeV LHC.

In Fig. 3, we have also analyzed different sources of uncertainties in these predictions.

In general, the scale uncertainties at NLO are around 20% which gets reduced to around 15% in NLO+NLL distribution, particularly in the high invariant mass region as shown in the left panel of Fig. 3. In contrast, the NSV resummation at NLO+NLL does not show similar scale reduction over NLO, particularly in the low invariant mass region. In the high invariant mass region, it marginally improves the scale uncertainty over the NLO results. In the bottom panels of Fig. 3, we compare the PDF uncertainties for both SV and NSV resummed cases against the fixed order. These uncertainties generally increase with Q as PDFs are well-constrained in the small- x region relevant to the ZH threshold production, whereas at large- x , these are poorly constrained resulting in significant uncertainties of around 10% at NLO in the high- Q region. The SV and NSV resummed results show marginal improvements in PDF uncertainties by around 0.8% over the NLO.

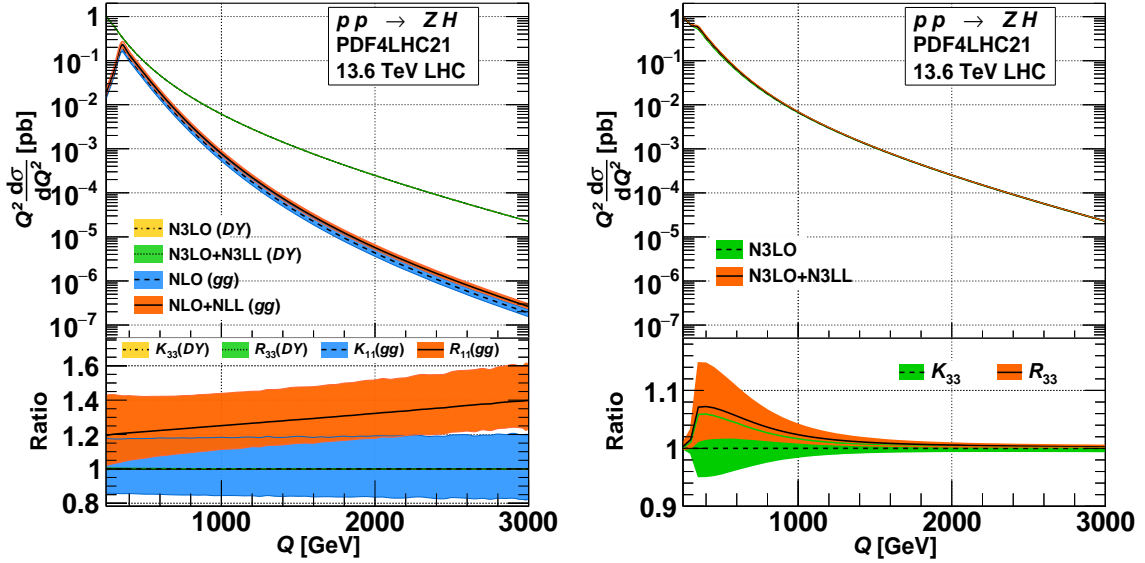


Figure 4: Left: The DY and gluon subprocesses contributions are shown for fixed order and SV resummed cases with the corresponding ratios at the bottom and its uncertainty from the scale variation. Right: The combined contribution at the highest accuracy for the fixed order and the SV resummed order are shown along with the scale uncertainties.

$$\begin{aligned}
 Q^2 \frac{d\sigma_{pp}^{\text{N3LO}}}{dQ^2} &= Q^2 \frac{d\sigma_{\text{DY}}^{\text{N3LO}}}{dQ^2} + Q^2 \frac{d\sigma_{gg}^{\text{NLO}}}{dQ^2}, \\
 Q^2 \frac{d\sigma_{pp}^{\text{N3LO+N3LL}}}{dQ^2} &= Q^2 \frac{d\sigma_{\text{DY}}^{\text{N3LO+N3LL}}}{dQ^2} + Q^2 \frac{d\sigma_{gg}^{\text{NLO+NLL}}}{dQ^2}.
 \end{aligned} \tag{3.2}$$

For completeness, we combine the gluon fusion results with other subprocesses for ZH contribution to obtain full $pp \rightarrow ZH$ results at $\mathcal{O}(\alpha_s^3)$ level. Particularly, in the fixed order case, we combine the contributions arising from the DY-type channel with that from the gluon fusion channel at $\mathcal{O}(\alpha_s^3)$ as given in Eq. (3.2). For resummation case, we chose to use the SV resummed results. While NSV resummation shows some enhancement over the SV resummed results (as seen from Fig. 2), it still lacks contributions from off-diagonal channels.

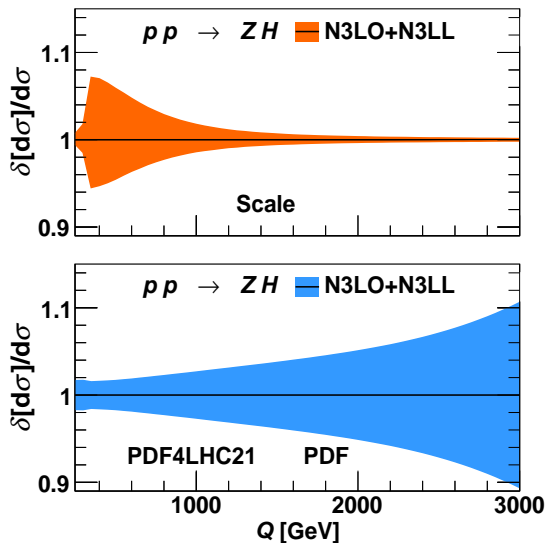


Figure 5: The 7-point scale uncertainty (upper panel) and the PDF uncertainty (lower panel) are shown for the $pp \rightarrow ZH$ process at 13.6 TeV LHC.

Moreover, one would also require the NSV accuracy for the DY-type subprocess for which the relevant ingredients are still missing. Hence we combine the fixed order results with SV resummed results for both DY-type and gluon fusion channels. The required N3LO+N3LL SV resummed results for the DY-type channel were obtained [82] by us a few years ago. In the left panel of Fig. 4, we show these results separately for both DY-type and gluon fusion channels along with the scale uncertainties. Note that the relative scale uncertainty for the DY-type is not visible on the scale of this plot. The right panel of Fig. 4 shows the combined results for invariant mass distribution at N3LO and N3LO+N3LL. The bottom panel highlights the enhancement from N3LO through the K_{33} and R_{33} factors. In Fig. 5, we show the scale and PDF uncertainties for the combined results at N3LO+N3LL. The PDF uncertainty increases with Q , reaching around 10.6% in the high invariant mass region. On the other hand, the scale uncertainty is largest at the top threshold ($Q \sim 2m_t$), reaching up to 6% and decreasing significantly in the high- Q region, reducing to as low as 0.1%.

3.2 Total cross-section

Finally, we also present the total cross-section for the resummed results by integrating the invariant mass distributions up to \sqrt{S} . The Table 1 provides the total cross-sections for the gluon fusion channel at fixed order and at SV and NSV resummation. Alongside, we also provide various uncertainties arising from 7-point scale variation, non-perturbative PDF set, and the variation of the strong coupling constant $\alpha_s(M_Z)$. For the later we consider a variation in the 1σ range leading to a variation in the range $\alpha_s^-(M_Z) = 0.1165$ and $\alpha_s^+(M_Z) = 0.1195$. With the central choice for $\alpha_s^c(M_Z) = 0.118$ same as the PDF, we obtain the final uncertainty through $\delta(\alpha_s) = \pm \max |\sigma(\alpha_s^\pm(M_Z)) - \sigma(\alpha_s^c(M_Z))| / \sigma(\alpha_s^c(M_Z))$. Additionally, we also present the combined uncertainties from PDF and α_s by adding

Order	cross-section (fb)	Scale	$\delta(\text{PDF})$	$\delta(\alpha_s)$	$\delta(\text{PDF} + \alpha_s)$
σ_{gg}^{LO}	60.25	$\pm 24.6\%$	$\pm 0.68\%$	$\pm 2.07\%$	$\pm 2.18\%$
σ_{gg}^{NLO}	124.74	$\pm 15.3\%$	$\pm 0.71\%$	$\pm 2.60\%$	$\pm 2.70\%$
$\sigma_{gg}^{\text{LO+LL}}$	84.74	$\pm 27.5\%$	$\pm 0.69\%$	$\pm 2.45\%$	$\pm 2.55\%$
$\sigma_{gg}^{\text{NLO+NLL}}$	151.30	$\pm 19.4\%$	$\pm 0.71\%$	$\pm 2.93\%$	$\pm 3.01\%$
$\sigma_{gg}^{\text{LO+LL}}$	96.27	$\pm 29.3\%$	$\pm 0.69\%$	$\pm 2.60\%$	$\pm 2.69\%$
$\sigma_{gg}^{\text{NLO+NLL}}$	170.73	$\pm 27.0\%$	$\pm 0.71\%$	$\pm 3.16\%$	$\pm 3.24\%$

Table 1: The ZH production cross-sections (in fb) are presented at exact LO, and Born-improved NLO, along with corresponding SV and NSV resummed results at 13.6 TeV LHC with 7-point scale, PDF and α_s uncertainties.

the respective errors in quadrature. The largest source of uncertainty arises from the scale variation which at NLO+NLL level are around 19.4%, indicating the need for further improvements through higher-order computation.

Order	cross-section (pb)	Scale	$\delta(\text{PDF})$	$\delta(\alpha_s)$	$\delta(\text{PDF} + \alpha_s)$
$\sigma_{\text{DY}}^{\text{N3LO}}$	0.8416	$\pm 0.28\%$	$\pm 0.77\%$	$\pm 0.14\%$	$\pm 0.78\%$
$\sigma_{\text{DY}}^{\text{N3LO+N3LL}}$	0.8416	$\pm 0.55\%$	$\pm 0.77\%$	$\pm 0.14\%$	$\pm 0.78\%$
$\sigma_{\text{tot}}^{\text{N3LO}}$	0.9776	$\pm 1.94\%$	$\pm 0.65\%$	$\pm 0.47\%$	$\pm 0.80\%$
$\sigma_{\text{tot}}^{\text{N3LO+N3LL}}$	1.0042	$\pm 2.98\%$	$\pm 0.63\%$	$\pm 0.58\%$	$\pm 0.86\%$

Table 2: ZH production cross-section (in pb) of DY-type N3LO, DY-type N3LO+N3LL, total N3LO and total resummed N3LO+N3LL which are defined in Eq. (3.3) for different 13.6 TeV LHC with 7-point scale, PDF and α_s uncertainties.

In Table 2, we present the total production cross-section of ZH at the LHC by combining contributions from different channels. Particularly, in the fixed order case, we combine the contributions arising from the DY-type channel ($\sigma_{\text{DY}}^{\text{N3LO}}$), the bottom-quark initiated t -channel ($\sigma_{b\bar{b}}$), the gluon fusion channel (σ_{gg}^{NLO}), and contribution coming from Higgs radiation from top quark loop in the quark annihilation channel ($\sigma_{\text{top}}(a_s^2)$) as described in Section 1 and defined in Eq. (3.3),

$$\begin{aligned}
\sigma_{\text{tot}}^{\text{N3LO}} &= \sigma_{\text{DY}}^{\text{N3LO}} + \sigma_{gg}^{\text{NLO}} + \sigma_{\text{top}}(a_s^2) + \sigma_{b\bar{b}}, \\
\sigma_{\text{tot}}^{\text{N3LO+N3LL}} &= \sigma_{\text{DY}}^{\text{N3LO+N3LL}} + \sigma_{gg}^{\text{NLO+NLL}} + \sigma_{\text{top}}(a_s^2) + \sigma_{b\bar{b}}.
\end{aligned} \tag{3.3}$$

For the resummation case, we improve the fixed order for the DY-type channel by SV resummation at N3LO+N3LL and for the gluon channel by resummation at NLO+NLL. For the DY-type channel, resummation has very little effect in this order and the major improvement is obtained through the gluon fusion channel. For the total cross-section, the resummation improves the cross-section by around 2.7% compared to the fixed order, whereas the scale uncertainty increases by 1%. This can be traced to the fact that, total cross-section receives significant contributions from the low invariant mass region, where the factorisation scale uncertainty remains significant. However, all other sources of uncertainties remain small, contributing less than 1%.

4 Conclusion

To summarize, we have investigated the impact of soft gluon resummation on the ZH production process in the gluon fusion channel at the LHC. In the low invariant mass region, near the top-pair threshold ($Q \sim 2m_t$), the gluon fusion channel at $\mathcal{O}(\alpha_s^2)$ level contributes around 20% of the dominant DY-type channel, highlighting its significance and the necessity of including its contribution.

We first obtained the Born improved NLO corrections by rescaling the exact LO results with the mass dependent NLO K-factor obtained from the Effective theory. Using the universal cusp anomalous dimensions, splitting kernels, we have performed the SV and the NSV resummation and presented numerical results for the invariant mass distribution as well as the production cross sections to NLO+NLL($\overline{\text{NLL}}$) accuracy for the current LHC energies. The NLO corrections contribute as large as 100% of LO for the total ZH production cross-section in the gluon fusion channel. We observed that the SV (NSV) resummation contributes an additional 19.4% (35.3%) at NLL ($\overline{\text{NLL}}$) level over NLO in the low Q -region. In the high invariant mass regions (around $Q = 3000$ GeV), this SV(NSV) resummation reduces the 7-point scale uncertainties at NLO level by a few percent 5.0%(1.4%). Besides the scale uncertainties, we have also quantified the uncertainties due to the PDFs on resummed results and these are found to be around 1.6% in the low invariant mass region.

Finally, for experimental analysis, we combine the contributions from different subprocesses, including the soft gluon resummation effects, and present comprehensive results for the invariant mass distribution as well as the total production cross sections at the LHC. We note that except for the uncertainties due to the non-perturbative inputs from PDFs, the theoretical uncertainties in the high invariant mass region are well under control. However, to advance the precision for this process further, the higher order corrections beyond NLO for the gluon fusion channel will be essential.

Acknowledgements

The research of G.D. is supported by the Deutsche Forschungsgemeinschaft (DFG, German Research Foundation) under grant 396021762 - TRR 257 (*Particle Physics Phenomenology after Higgs discovery*). The research work of M.C.K. is supported by the SERB Core Research Grant (CRG) under the project CRG/2021/005270. The research work of K.S.

is supported by the Royal Society (URF/R/231031) and the STFC (ST/X003167/1 and ST/X000745/1). The computation has been performed on the OMNI cluster at the University of Siegen, and on the PARAM ISHAN cluster computing facility at IIT Guwahati. We thank Pulak Banerjee for the useful discussion. G.D. also thanks Aparna Sankar for helpful communication.

References

- [1] F. Englert and R. Brout, *Broken Symmetry and the Mass of Gauge Vector Mesons*, *Phys. Rev. Lett.* **13** (1964) 321.
- [2] P. W. Higgs, *Broken Symmetries and the Masses of Gauge Bosons*, *Phys. Rev. Lett.* **13** (1964) 508.
- [3] G. S. Guralnik, C. R. Hagen and T. W. B. Kibble, *Global Conservation Laws and Massless Particles*, *Phys. Rev. Lett.* **13** (1964) 585.
- [4] ATLAS collaboration, G. Aad et al., *Observation of a new particle in the search for the Standard Model Higgs boson with the ATLAS detector at the LHC*, *Phys. Lett. B* **716** (2012) 1 [1207.7214].
- [5] CMS collaboration, S. Chatrchyan et al., *Observation of a New Boson at a Mass of 125 GeV with the CMS Experiment at the LHC*, *Phys. Lett. B* **716** (2012) 30 [1207.7235].
- [6] C. Englert, M. McCullough and M. Spannowsky, *Gluon-initiated associated production boosts Higgs physics*, *Phys. Rev. D* **89** (2014) 013013 [1310.4828].
- [7] B. Hespel, F. Maltoni and E. Vryonidou, *Higgs and Z boson associated production via gluon fusion in the SM and the 2HDM*, *JHEP* **06** (2015) 065 [1503.01656].
- [8] D. Goncalves, F. Krauss, S. Kuttimalai and P. Maierhöfer, *Higgs-Strahlung: Merging the NLO Drell-Yan and Loop-Induced 0+1 jet Multiplicities*, *Phys. Rev. D* **92** (2015) 073006 [1509.01597].
- [9] ATLAS collaboration, M. Aaboud et al., *Measurement of VH , $H \rightarrow b\bar{b}$ production as a function of the vector-boson transverse momentum in 13 TeV pp collisions with the ATLAS detector*, *JHEP* **05** (2019) 141 [1903.04618].
- [10] ATLAS collaboration, G. Aad et al., *Measurement of the associated production of a Higgs boson decaying into b-quarks with a vector boson at high transverse momentum in pp collisions at $\sqrt{s} = 13$ TeV with the ATLAS detector*, *Phys. Lett. B* **816** (2021) 136204 [2008.02508].
- [11] ATLAS collaboration, G. Aad et al., *Measurements of WH and ZH production in the $H \rightarrow b\bar{b}$ decay channel in pp collisions at 13 TeV with the ATLAS detector*, *Eur. Phys. J. C* **81** (2021) 178 [2007.02873].
- [12] CMS collaboration, *Combined Higgs boson production and decay measurements with up to 137 fb⁻¹ of proton-proton collision data at $\sqrt{s} = 13$ TeV*, .
- [13] ATLAS collaboration, *Combination of measurements of Higgs boson production in association with a W or Z boson in the $b\bar{b}$ decay channel with the ATLAS experiment at $\sqrt{s} = 13$ TeV*, .

- [14] CMS collaboration, V. Chekhovsky et al., *Constraints on standard model effective field theory for a Higgs boson produced in association with W or Z bosons in the $H \rightarrow b\bar{b}$ decay channel in proton-proton collisions at $\sqrt{s} = 13$ TeV*, [2411.16907](#).
- [15] CMS collaboration, A. Hayrapetyan et al., *Study of WH production through vector boson scattering and extraction of the relative sign of the W and Z couplings to the Higgs boson in proton-proton collisions at $\sqrt{s} = 13$ TeV*, [2405.16566](#).
- [16] CMS collaboration, A. Hayrapetyan et al., *Search for ZZ and ZH production in the $b\bar{b}b\bar{b}$ final state using proton-proton collisions at $\sqrt{s} = 13$ TeV*, *Eur. Phys. J. C* **84** (2024) 712 [[2403.20241](#)].
- [17] CMS collaboration, A. Hayrapetyan et al., *Search for Higgs boson pair production with one associated vector boson in proton-proton collisions at $\sqrt{s} = 13$ TeV*, *JHEP* **10** (2024) 061 [[2404.08462](#)].
- [18] CMS collaboration, A. Tumasyan et al., *Measurement of simplified template cross sections of the Higgs boson produced in association with W or Z bosons in the $H \rightarrow b\bar{b}$ decay channel in proton-proton collisions at $s=13$ TeV*, *Phys. Rev. D* **109** (2024) 092011 [[2312.07562](#)].
- [19] ATLAS collaboration, G. Aad et al., *Measurements of WH and ZH production with Higgs boson decays into bottom quarks and direct constraints on the charm Yukawa coupling in 13 TeV pp collisions with the ATLAS detector*, [2410.19611](#).
- [20] T. Han and S. Willenbrock, *QCD correction to the $pp \rightarrow WH$ and ZH total cross-sections*, *Phys. Lett. B* **273** (1991) 167.
- [21] O. Brein, A. Djouadi and R. Harlander, *NNLO QCD corrections to the Higgs-strahlung processes at hadron colliders*, *Phys. Lett. B* **579** (2004) 149 [[hep-ph/0307206](#)].
- [22] O. Brein, M. Ciccolini, S. Dittmaier, A. Djouadi, R. Harlander and M. Kramer, *Precision calculations for associated WH and ZH production at hadron colliders*, in *3rd Les Houches Workshop on Physics at TeV Colliders*, 2, 2004, [hep-ph/0402003](#).
- [23] O. Brein, R. V. Harlander and T. J. E. Zirke, *vh@nnlo - Higgs Strahlung at hadron colliders*, *Comput. Phys. Commun.* **184** (2013) 998 [[1210.5347](#)].
- [24] G. Ferrera, M. Grazzini and F. Tramontano, *Associated ZH production at hadron colliders: the fully differential NNLO QCD calculation*, *Phys. Lett. B* **740** (2015) 51 [[1407.4747](#)].
- [25] J. M. Campbell, R. K. Ellis and C. Williams, *Associated production of a Higgs boson at NNLO*, *JHEP* **06** (2016) 179 [[1601.00658](#)].
- [26] G. Ferrera, G. Somogyi and F. Tramontano, *Associated production of a Higgs boson decaying into bottom quarks at the LHC in full NNLO QCD*, *Phys. Lett. B* **780** (2018) 346 [[1705.10304](#)].
- [27] R. V. Harlander, J. Klappert, S. Liebler and L. Simon, *vh@nnlo-v2: New physics in Higgs Strahlung*, *JHEP* **05** (2018) 089 [[1802.04817](#)].
- [28] J. Baglio, C. Duhr, B. Mistlberger and R. Szafron, *Inclusive Production Cross Sections at N3LO*, [2209.06138](#).
- [29] T. Ahmed, A. H. Ajjath, L. Chen, P. K. Dhani, P. Mukherjee and V. Ravindran, *Polarised Amplitudes and Soft-Virtual Cross Sections for $b\bar{b} \rightarrow ZH$ at NNLO in QCD*, *JHEP* **01** (2020) 030 [[1910.06347](#)].

- [30] M. L. Ciccolini, S. Dittmaier and M. Kramer, *Electroweak radiative corrections to associated WH and ZH production at hadron colliders*, *Phys. Rev. D* **68** (2003) 073003 [[hep-ph/0306234](#)].
- [31] A. Denner, S. Dittmaier, S. Kallweit and A. Muck, *Electroweak corrections to Higgs-strahlung off W/Z bosons at the Tevatron and the LHC with HAWK*, *JHEP* **03** (2012) 075 [[1112.5142](#)].
- [32] O. Brein, R. Harlander, M. Wiesemann and T. Zirke, *Top-Quark Mediated Effects in Hadronic Higgs-Strahlung*, *Eur. Phys. J. C* **72** (2012) 1868 [[1111.0761](#)].
- [33] D. A. Dicus and C. Kao, *Higgs Boson - Z⁰ Production From Gluon Fusion*, *Phys. Rev. D* **38** (1988) 1008.
- [34] B. A. Kniehl and C. P. Palisoc, *Associated production of Z and neutral Higgs bosons at the CERN Large Hadron Collider*, *Phys. Rev. D* **85** (2012) 075027 [[1112.1575](#)].
- [35] L. Altenkamp, S. Dittmaier, R. V. Harlander, H. Rzehak and T. J. E. Zirke, *Gluon-induced Higgs-strahlung at next-to-leading order QCD*, *JHEP* **02** (2013) 078 [[1211.5015](#)].
- [36] A. Hasselhuhn, T. Luthe and M. Steinhauser, *On top quark mass effects to gg → ZH at NLO*, *JHEP* **01** (2017) 073 [[1611.05881](#)].
- [37] J. Davies, G. Mishima and M. Steinhauser, *Virtual corrections to gg → ZH in the high-energy and large-m_t limits*, *JHEP* **03** (2021) 034 [[2011.12314](#)].
- [38] L. Alasfar, G. Degrassi, P. P. Giardino, R. Gröber and M. Vitti, *Virtual corrections to gg → ZH via a transverse momentum expansion*, *JHEP* **05** (2021) 168 [[2103.06225](#)].
- [39] L. Bellafronte, G. Degrassi, P. P. Giardino, R. Groeber and M. Vitti, *Gluon fusion production at NLO: merging the transverse momentum and the high-energy expansions*, *JHEP* **07** (2022) 069 [[2202.12157](#)].
- [40] G. Degrassi, R. Gröber, M. Vitti and X. Zhao, *On the NLO QCD corrections to gluon-initiated ZH production*, *JHEP* **08** (2022) 009 [[2205.02769](#)].
- [41] G. Wang, X. Xu, Y. Xu and L. L. Yang, *Next-to-leading order corrections for gg → ZH with top quark mass dependence*, *Phys. Lett. B* **829** (2022) 137087 [[2107.08206](#)].
- [42] L. Chen, G. Heinrich, S. P. Jones, M. Kerner, J. Klappert and J. Schlenk, *ZH production in gluon fusion: two-loop amplitudes with full top quark mass dependence*, *JHEP* **03** (2021) 125 [[2011.12325](#)].
- [43] L. Chen, J. Davies, G. Heinrich, S. P. Jones, M. Kerner, G. Mishima et al., *ZH production in gluon fusion at NLO in QCD*, *JHEP* **08** (2022) 056 [[2204.05225](#)].
- [44] G. F. Sterman, *Summation of Large Corrections to Short Distance Hadronic Cross-Sections*, *Nucl. Phys. B* **281** (1987) 310.
- [45] S. Catani and L. Trentadue, *Resummation of the QCD Perturbative Series for Hard Processes*, *Nucl. Phys. B* **327** (1989) 323.
- [46] S. Catani and L. Trentadue, *Comment on QCD exponentiation at large x*, *Nucl. Phys. B* **353** (1991) 183.
- [47] S. Moch, J. A. M. Vermaseren and A. Vogt, *Higher-order corrections in threshold resummation*, *Nucl. Phys. B* **726** (2005) 317 [[hep-ph/0506288](#)].
- [48] E. Laenen and L. Magnea, *Threshold resummation for electroweak annihilation from DIS data*, *Phys. Lett. B* **632** (2006) 270 [[hep-ph/0508284](#)].

- [49] V. Ravindran, *On Sudakov and soft resummations in QCD*, *Nucl. Phys. B* **746** (2006) 58 [[hep-ph/0512249](#)].
- [50] V. Ravindran, *Higher-order threshold effects to inclusive processes in QCD*, *Nucl. Phys. B* **752** (2006) 173 [[hep-ph/0603041](#)].
- [51] A. Idilbi, X.-d. Ji and F. Yuan, *Resummation of threshold logarithms in effective field theory for DIS, Drell-Yan and Higgs production*, *Nucl. Phys. B* **753** (2006) 42 [[hep-ph/0605068](#)].
- [52] T. Becher, M. Neubert and B. D. Pecjak, *Factorization and Momentum-Space Resummation in Deep-Inelastic Scattering*, *JHEP* **01** (2007) 076 [[hep-ph/0607228](#)].
- [53] T. Ahmed, A. H. Ajjath, G. Das, P. Mukherjee, V. Ravindran and S. Tiwari, *Soft-virtual correction and threshold resummation for n-colorless particles to fourth order in QCD: Part I*, [2010.02979](#).
- [54] S. Catani, D. de Florian, M. Grazzini and P. Nason, *Soft gluon resummation for Higgs boson production at hadron colliders*, *JHEP* **07** (2003) 028 [[hep-ph/0306211](#)].
- [55] S. Moch and A. Vogt, *Higher-order soft corrections to lepton pair and Higgs boson production*, *Phys. Lett. B* **631** (2005) 48 [[hep-ph/0508265](#)].
- [56] D. de Florian and J. Zurita, *Soft-gluon resummation for pseudoscalar Higgs boson production at hadron colliders*, *Phys. Lett. B* **659** (2008) 813 [[0711.1916](#)].
- [57] S. Catani, L. Cieri, D. de Florian, G. Ferrera and M. Grazzini, *Threshold resummation at N^3LL accuracy and soft-virtual cross sections at N^3LO* , *Nucl. Phys. B* **888** (2014) 75 [[1405.4827](#)].
- [58] M. Bonvini and S. Marzani, *Resummed Higgs cross section at N^3LL* , *JHEP* **09** (2014) 007 [[1405.3654](#)].
- [59] T. Ahmed, G. Das, M. C. Kumar, N. Rana and V. Ravindran, *RG improved Higgs boson production to N^3LO in QCD*, [1505.07422](#).
- [60] T. Schmidt and M. Spira, *Higgs Boson Production via Gluon Fusion: Soft-Gluon Resummation including Mass Effects*, *Phys. Rev. D* **93** (2016) 014022 [[1509.00195](#)].
- [61] T. Ahmed, M. Bonvini, M. C. Kumar, P. Mathews, N. Rana, V. Ravindran et al., *Pseudo-scalar Higgs boson production at $N^3 LO_A + N^3 LL'$* , *Eur. Phys. J. C* **76** (2016) 663 [[1606.00837](#)].
- [62] M. Bonvini, S. Marzani, C. Muselli and L. Rottoli, *On the Higgs cross section at N^3LO+N^3LL and its uncertainty*, *JHEP* **08** (2016) 105 [[1603.08000](#)].
- [63] A. A H, A. Chakraborty, G. Das, P. Mukherjee and V. Ravindran, *Resummed prediction for Higgs boson production through $b\bar{b}$ annihilation at N^3LL* , *JHEP* **11** (2019) 006 [[1905.03771](#)].
- [64] G. Das, S.-O. Moch and A. Vogt, *Soft corrections to inclusive deep-inelastic scattering at four loops and beyond*, *JHEP* **03** (2020) 116 [[1912.12920](#)].
- [65] G. Das, M. C. Kumar and K. Samanta, *Resummed inclusive cross-section in ADD model at N^3LL* , *JHEP* **10** (2020) 161 [[1912.13039](#)].
- [66] G. Das, M. C. Kumar and K. Samanta, *Resummed inclusive cross-section in Randall-Sundrum model at NNLO+NNLL*, *JHEP* **07** (2020) 040 [[2004.03938](#)].
- [67] G. Das, M. C. Kumar and K. Samanta, *Precision QCD phenomenology of exotic spin-2 search at the LHC*, *JHEP* **04** (2021) 111 [[2011.15121](#)].

- [68] A. A H, G. Das, M. C. Kumar, P. Mukherjee, V. Ravindran and K. Samanta, *Resummed Drell-Yan cross-section at N^3LL* , *JHEP* **10** (2020) 153 [2001.11377].
- [69] P. Banerjee, C. Dey, M. C. Kumar and V. Pandey, *Threshold resummation for Z-boson pair production at NNLO+NNLL*, 2409.16375.
- [70] S. Moch and A. Vogt, *On non-singlet physical evolution kernels and large-x coefficient functions in perturbative QCD*, *JHEP* **11** (2009) 099 [0909.2124].
- [71] G. Soar, S. Moch, J. A. M. Vermaseren and A. Vogt, *On Higgs-exchange DIS, physical evolution kernels and fourth-order splitting functions at large x*, *Nucl. Phys. B* **832** (2010) 152 [0912.0369].
- [72] D. Bonocore, E. Laenen, L. Magnea, S. Melville, L. Vernazza and C. D. White, *A factorization approach to next-to-leading-power threshold logarithms*, *JHEP* **06** (2015) 008 [1503.05156].
- [73] V. Del Duca, E. Laenen, L. Magnea, L. Vernazza and C. D. White, *Universality of next-to-leading power threshold effects for colourless final states in hadronic collisions*, *JHEP* **11** (2017) 057 [1706.04018].
- [74] N. Bahjat-Abbas, D. Bonocore, J. Sinninghe Damsté, E. Laenen, L. Magnea, L. Vernazza et al., *Diagrammatic resummation of leading-logarithmic threshold effects at next-to-leading power*, *JHEP* **11** (2019) 002 [1905.13710].
- [75] M. Beneke, A. Broggio, S. Jaskiewicz and L. Vernazza, *Threshold factorization of the Drell-Yan process at next-to-leading power*, *JHEP* **07** (2020) 078 [1912.01585].
- [76] M. van Beekveld, W. Beenakker, R. Basu, E. Laenen, A. Misra and P. Motylinski, *Next-to-leading power threshold effects for resummed prompt photon production*, *Phys. Rev. D* **100** (2019) 056009 [1905.11771].
- [77] G. Das, S. Moch and A. Vogt, *Approximate four-loop QCD corrections to the Higgs-boson production cross section*, *Phys. Lett. B* **807** (2020) 135546 [2004.00563].
- [78] A. A H, P. Mukherjee and V. Ravindran, *Next to soft corrections to Drell-Yan and Higgs boson productions*, *Phys. Rev. D* **105** (2022) 094035 [2006.06726].
- [79] A. A H, P. Mukherjee, V. Ravindran, A. Sankar and S. Tiwari, *Resummed Higgs boson cross section at next-to SV to NNLO + NNLL*, *Eur. Phys. J. C* **82** (2022) 774 [2109.12657].
- [80] M. van Beekveld, E. Laenen, J. Sinninghe Damsté and L. Vernazza, *Next-to-leading power threshold corrections for finite order and resummed colour-singlet cross sections*, *JHEP* **05** (2021) 114 [2101.07270].
- [81] A. A H, P. Mukherjee and V. Ravindran, *Going beyond soft plus virtual*, *Phys. Rev. D* **105** (2022) L091503 [2204.09012].
- [82] G. Das, C. Dey, M. C. Kumar and K. Samanta, *Threshold enhanced cross sections for colorless productions*, *Phys. Rev. D* **107** (2023) 034038 [2210.17534].
- [83] R. V. Harlander, A. Kulesza, V. Theeuwes and T. Zirke, *Soft gluon resummation for gluon-induced Higgs Strahlung*, *JHEP* **11** (2014) 082 [1410.0217].
- [84] S. Moch, J. A. M. Vermaseren and A. Vogt, *The Three loop splitting functions in QCD: The Nonsinglet case*, *Nucl. Phys. B* **688** (2004) 101 [hep-ph/0403192].
- [85] A. Vogt, S. Moch and J. A. M. Vermaseren, *The Three-loop splitting functions in QCD: The Singlet case*, *Nucl. Phys. B* **691** (2004) 129 [hep-ph/0404111].

- [86] V. V. Sudakov, *Vertex parts at very high-energies in quantum electrodynamics*, *Sov. Phys. JETP* **3** (1956) 65.
- [87] A. H. Mueller, *On the Asymptotic Behavior of the Sudakov Form-factor*, *Phys. Rev. D* **20** (1979) 2037.
- [88] J. C. Collins, *Algorithm to Compute Corrections to the Sudakov Form-factor*, *Phys. Rev. D* **22** (1980) 1478.
- [89] A. Sen, *Asymptotic Behavior of the Sudakov Form-Factor in QCD*, *Phys. Rev. D* **24** (1981) 3281.
- [90] A. A H, P. Mukherjee, V. Ravindran, A. Sankar and S. Tiwari, *Next-to SV resummed Drell–Yan cross section beyond leading-logarithm*, *Eur. Phys. J. C* **82** (2022) 234 [2107.09717].
- [91] M. van Beekveld, L. Vernazza and C. D. White, *Threshold resummation of new partonic channels at next-to-leading power*, *JHEP* **12** (2021) 087 [2109.09752].
- [92] S. Catani, M. L. Mangano, P. Nason and L. Trentadue, *The Resummation of soft gluons in hadronic collisions*, *Nucl. Phys. B* **478** (1996) 273 [hep-ph/9604351].
- [93] A. Vogt, *Efficient evolution of unpolarized and polarized parton distributions with QCD-PEGASUS*, *Comput. Phys. Commun.* **170** (2005) 65 [hep-ph/0408244].
- [94] PDF4LHC WORKING GROUP collaboration, R. D. Ball et al., *The PDF4LHC21 combination of global PDF fits for the LHC Run III*, *J. Phys. G* **49** (2022) 080501 [2203.05506].
- [95] A. Buckley, J. Ferrando, S. Lloyd, K. Nordström, B. Page, M. Rüfenacht et al., *LHAPDF6: parton density access in the LHC precision era*, *Eur. Phys. J. C* **75** (2015) 132 [1412.7420].
- [96] PARTICLE DATA GROUP collaboration, S. Navas et al., *Review of particle physics*, *Phys. Rev. D* **110** (2024) 030001.